Journal of Power Sources 233 (2013) 110–114

Contents lists available at SciVerse ScienceDirect

Journal of Power Sources

journal homepage: www.elsevier.com/locate/jpowsour

Short communication

SEI investigations on copper electrodes after lithium plating with Raman spectroscopy and mass spectrometry

René Schmitz*, Romek Ansgar Müller, Raphael Wilhelm Schmitz, Christian Schreiner, Miriam Kunze, Alexandra Lex-Balducci, Stefano Passerini, Martin Winter

Westfälische Wilhelms-Universität Münster, Institute of Physical Chemistry, MEET Battery Research Center, Corrensstr. 46, 48149 Muenster, Germany

HIGHLIGHTS

- The SEI on deposited Lithium metal was investigated by Raman and mass spectrometry.
- Li_2C_2 was detected as one of the main components.
- The distribution of Li_2C_2 and Li_2CO_3 on the surface was studied by Raman mapping.
- A special *in situ* Raman method was developed to investigate the SEI-formation.
- *In situ* experiments showed that Li_2C_2 is formed at potentials below 0 V vs. Li/Li^+.

ARTICLE INFO

Article history:
Received 16 September 2012
Received in revised form
28 December 2012
Accepted 16 January 2013
Available online 26 January 2013

Keywords:
SEI
Raman
SERS
Raman mapping
Mass spectrometry
Lithium

ABSTRACT

The composition and formation of the SEI which is formed on lithium, which has been electrochemically deposited on a Cu substrate, is investigated by Raman spectroscopy and mass spectrometry. Semi-carbonates, Li_2CO_3 and Li_2C_2 are identified as SEI components. The existence of Li_2C_2 is further proven with mass spectrometry by analyzing the gases which are formed by hydrolysis. Raman mapping reveals that Li_2CO_3 is homogeneously distributed over the copper substrate, on which lithium was deposited. At contrast, Li_2C_2 is mainly located on the plated lithium. An *in situ* Raman spectroscopy method for SEI investigation was developed and shows that Li_2C_2 is not formed at a potential >0 V vs. Li/Li^+.

1. Introduction

Unlike lithium ion batteries [1–3], lithium metal batteries do not show the same reversibility and thus rechargeability [4]. However, lithium metal possesses unique features, when used as battery anode. Lithium has a high theoretical capacity of 3862 mAh g^{-1} and creates the lowest standard reference potential of all elements, when immersed in an appropriate electrolyte solution. Thus, high specific energies are achieved when lithium negative electrodes are combined with positive electrodes, that serve as lithium sink. However, in the rechargeable mode lithium metal anode based battery cells, present a safety hazard due to formation of reactive, high surface area dendrites [5]. Many efforts have been taken to improve rechargeable Li metal systems based on liquid organic electrolytes, but so far did not succeed [6–11]. The Solid Electrolyte Interphase (SEI) [12–14] composition has a strong impact the anode performance and this is especially true for metallic Li the lithium metal cycling behavior. The SEI basically consists of electrolyte decomposition products [LiF, Li_2CO_3, Semicarbonates, etc.] and is thus strongly influenced by the used electrolyte [15,16]. It forms immediately, when the electrolyte gets in contact with the highly reducing lithium metal electrode [12]. To study the composition of the SEI it is quite common to use *ex situ* XPS and for the reactions of SEI formation *in situ* by FT-IR spectroscopy [17,18].

Here, we show investigations on the SEI of electrochemically deposited lithium metal by *in situ* as well as *ex situ* by Raman spectroscopy and in addition with the help by *ex situ* mass spectrometry. Lithium metal is a favorable Raman substrate since it

* Corresponding author.
E-mail address: rene.schmitz@wwu.de (R. Schmitz).

0378-7753/$ – see front matter © 2013 Elsevier B.V. All rights reserved.
http://dx.doi.org/10.1016/j.jpowsour.2013.01.105

might result in a surface enhancement effect during the Raman spectroscopic experiment (SERS) [19,20]. This surface effect might lead to an enhancement of the Raman signals representing the SEI by a factor of up to 10^6 [21]. To investigate the local distribution of the SEI products, a Raman mapping has been carried out on the copper substrate on which lithium was plated. To understand at which potential the SEI products has been formed, an *in situ* Raman experiment has been done on the copper electrode. The copper substrate shows also a good surface enhancement factor at a laser wavelength of 785 cm^{-1} [19,20]. This SERS effect will help to detect even small amounts of SEI products also for the *in situ* measurement.

2. Experimental

2.1. Electrochemical lithium plating on copper

The electrochemical measurements were carried out with a multichannel VSP potentiostat (BioLogic). The electrochemical cell was constructed in a three electrode arrangement with lithium as reference and counter electrode. The copper foil was ultrasonically cleaned and washed with water and ethanol before use. A galvanostatic method with a current density of 0.1 mA cm^{-2} was applied for 1 h in order to deposit the lithium on the copper electrode. The cell was then disassembled and without further treatment the electrode was directly transferred to the (custom made) Raman cell or alternatively for hydrolysis in a (custom made) special mass spectrometry cell. As electrolyte, a solution of 1 M $LiPF_6$ in a mixture of ethylene carbonate (EC) and diethyl carbonate (DEC) (3:7 by weight) was used.

2.2. Raman spectroscopy

A Bruker SENTERRA dispersive Raman microscope was used to analyze the samples. The laser source was a green semiconductor-laser with 532 nm for the *ex situ* measurements. The laser power was adjusted by a filter to 5 mW. A grating of 400 lines mm^{-1} was used. For the microscope, a 10× objective was used. To collect the spectra, 5 integrations were carried out with an integration time of 5 s. For the Raman mapping a surface of 40 × 40 μm was probed with a distance of 2 μm between each measurement point.

For the *in situ* Raman measurement a special custom made *in situ* cell was used (cf. Fig. 1). The Raman microscope was directly focused on the copper working electrode (2 mm diameter) through the glass window (10 μm thick). The copper working electrode received a potentiodynamic sweep with a scan rate of 1 mV s^{-1} starting from the open circuit potential (OCP) to a selected cut-off potential (1.5 V, 1.0 V, 0.5 V, 0.1 V, 0 V and −0.1 V vs. Li/Li^+, respectively). When the selected potential was reached, the working electrode potential was held constant for 10 min. Subsequently, the Raman measurement was carried out with a 785 nm laser to enable the surface enhancement of copper. The laser power was set to 50 mW and the acquisition of the spectrum was done with 10 scans and an integration time of 1 s.

2.3. Mass spectrometry

A quadrupole mass spectrometer Prisma QMS 200 M (Pfeiffer Vacuum) recorded the mass to charge ratio (m/z) signals. A flow meter red-y compact (Voegtlin Instruments) controlled the argon carrier gas flow to 1.6 mL min^{-1} through the sample chamber which was connected by a stainless steal capillary to the online MS-cell. Millipore water was used for the hydrolysis. The water was purged with argon to eliminate CO_2 as a possible carbon source from the water.

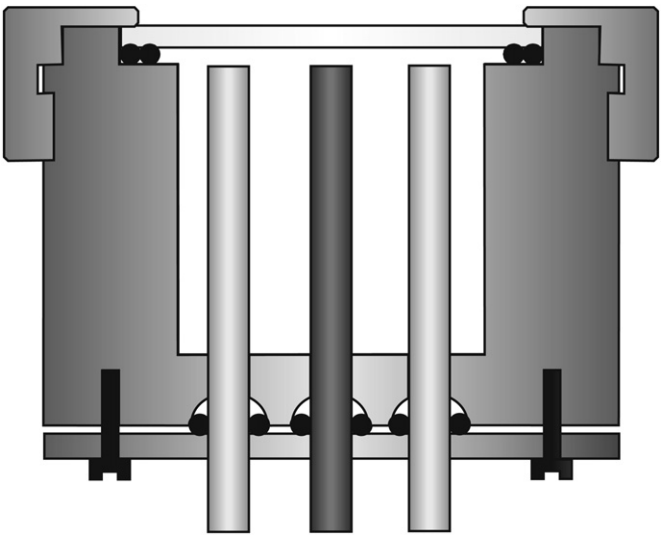

Fig. 1. Schematic depiction of the custom made *in situ* Raman cell. The cell setup is a three electrode arrangement with a copper working electrode in the middle and metallic lithium as counter and reference electrode. The Raman laser passes the glass window and is focused on the surface of the copper electrode.

3. Results and discussion

In the galvanostatic measurement the first faradaic reaction is observed at a potential of 1.2 V vs. Li/Li^+ (cf. Fig. 2). This reaction can be assigned to the reduction of organic carbonates. After this reduction the potential decreases further until an overpotential of −35 mV vs. Li/Li^+ is reached. At this potential, the deposition of metallic lithium starts. The deposition of lithium metal normally occurs inhomogeneously [9] and dendrites are formed on the copper surface which also can be observed in this study. A microscope picture of the copper electrode after lithium deposition is shown in Fig. 3. The dark spots on the copper electrode are lithium metal deposits. Apparently, lithium metal deposition is not uniform, but happens only locally.

Two single representative Raman spectra of the copper electrode are shown in Fig. 4. Spectrum 1 was measured at position 1 in Fig. 3 and spectrum 2 was measured at position 2. The spectra only differ in a signal at 1856 cm^{-1} which is only observed at position No. 1, where lithium is deposited. This signal can be assigned to the symmetric stretching vibration of Li_2C_2 [22], which results from the stretching of the triple bond of the acetylide anion [23].

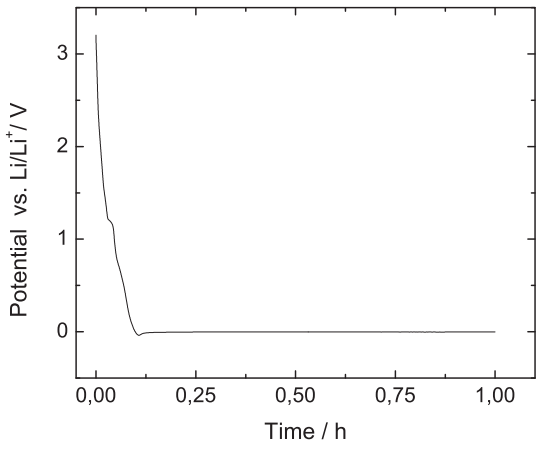

Fig. 2. Potential vs. time plot of a galvanostatic reduction process on a copper working electrode in 1 M $LiPF_6$ in EC:DEC (3:7 by wt.). The current density was 0.1 mA cm^{-2}, both, counter and reference electrode consisted of lithium metal.

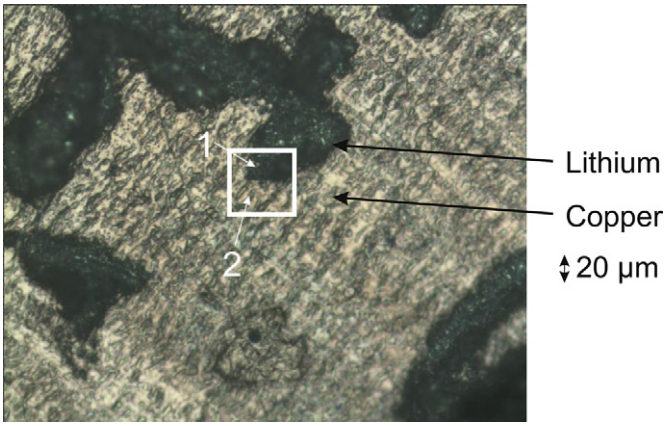

Fig. 3. Microscopic picture (10× magnification) of the copper foil after lithium deposition.

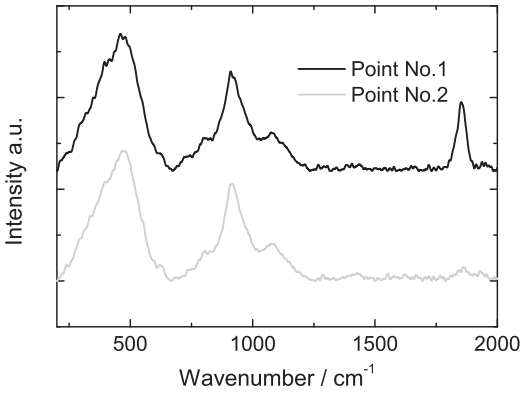

Fig. 4. Raman spectra of position one and position two on the copper electrode.

The existence of Li_2C_2 is also in good agreement with the slight turquoise color of the lithium deposits on the copper foil (cf. Fig. 3). When an excess of lithium metal is present, Li_2C_2 shows a bluish color which results most likely from color centers (F-centers) [23]. Color centers are structural defects in crystals where electrons substitute anions. In addition to the signal at 1856 cm^{-1}, other signals were detected on the copper foil. The signal at 1080 cm^{-1} which is present in both spectra can be assigned to the symmetric stretching vibration of the carbonate anion from Li_2CO_3 [24]. Li_2CO_3 is an SEI product stemming from decomposition of the organic carbonates in the electrolyte [15]. The broad signal at 920 cm^{-1} cannot be clearly assigned to one SEI-component. There are several possible explanations for this broad signal. On the one hand, these signals could originate from the nondecomposed electrolyte itself. At these wavenumbers, ring breathing modes of EC-lithium complexes [25] R–O and C–C stretching modes [26] of the solvents can be observed in the Raman spectrum of the electrolyte.

Alternatively, this signal can be assigned to SEI products stemming from the decomposition of the carbonates, for instance semicarbonates, which are known as SEI products [15]. In this case the signal at 920 cm^{-1} would occur because of the stretching vibrations of R–O– and C–C–bonds in the semicarbonates.

A further signal is observed at 470 cm^{-1} which is again very broad. This signal can be assigned to deformation vibrations of the SEI compounds that also cause the signal at 920 cm^{-1}.

To understand the composition and distribution of these SEI-products, which were discussed above, Raman mapping of the copper substrate with the deposited Li metal was carried out. With Raman mapping it is possible to investigate the distribution of the SEI products on the surface and to get information about their relative quantity. For each spectrum the integral of the specific peak signals was calculated. For the Raman mapping we focused on two signals. One is the signal of Li_2C_2 at 1856 cm^{-1} and the other one is the signal of the carbonate anion at 1080 cm^{-1}. The results are shown in Figs. 5 and 6.

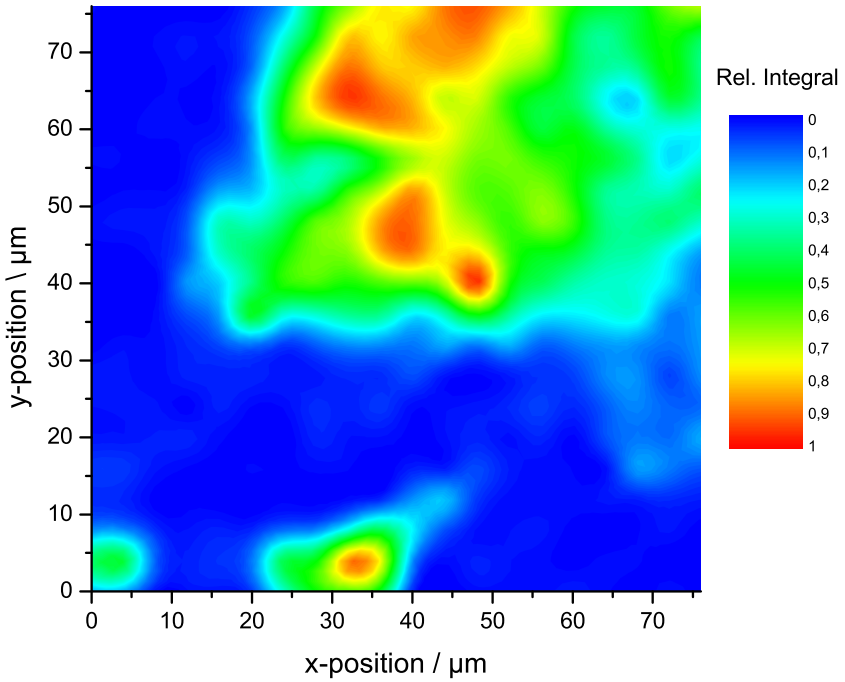

Fig. 5. Raman mapping of the signal at 1856 cm^{-1} (Li_2C_2) of a selected surface part of a copper foil on which lithium was electrodeposited. High integral values are shown in red, whereas low integral values and zero values, respectively, are shown in blue. The *x* and *y* axis represent the relative position where the spectrum was collected. (For interpretation of the references to color in this figure legend, the reader is referred to the web version of this article.)

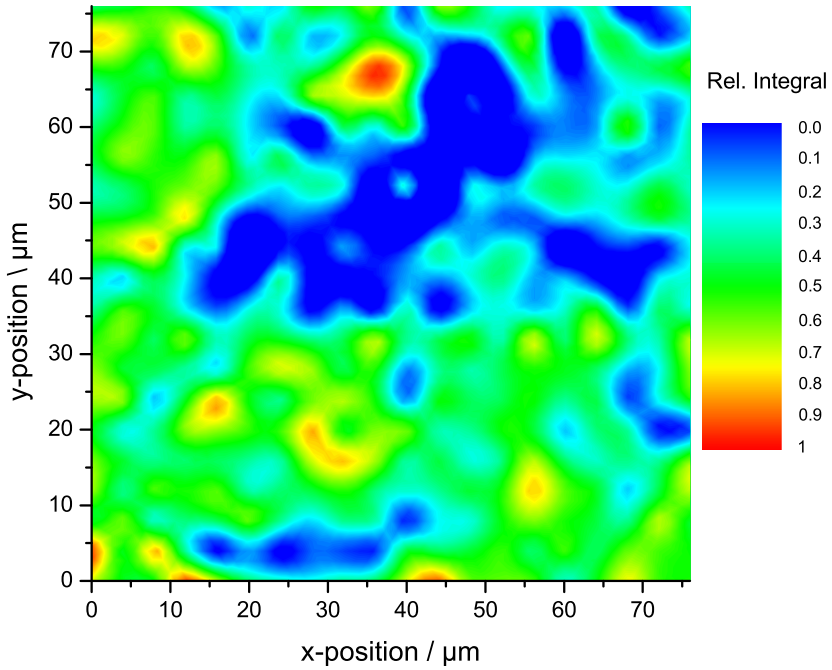

Fig. 6. Raman mapping of the signal at 1080 cm^{-1} (Li_2CO_3) of a selected surface part of a copper foil on which lithium was electrodeposited. The integral of the peak at is represented here. High integral values are shown in red whereas low integral values respectively zero values are shown in blue. The *x* and *y* axis represent the position where the spectrum was collected. (For interpretation of the references to colour in this figure legend, the reader is referred to the web version of this article.)

From the Raman mapping it becomes obvious that the SEI compound Li_2C_2 is inhomogeneously distributed over the copper substrate. The highest amount of Li_2C_2 was found on positions where lithium metal was plated and at the black and turquoise spots on the copper electrode, respectively (for comparison, cf. Fig. 3). However, the comparison of Figs. 3 and 5 shows that also at positions where the copper foil is not covered with black or turquoise colored products, Li_2C_2 can be found but in this case, the signals are weaker and thus low integral values are observed. Therefore, it can be concluded that Li_2C_2 is a major part of the SEI but does not cover the whole copper electrode. It is mainly formed at sites where massive plating of metallic lithium occurs. The presence of lithium metal on the electrode surface obviously causes the formation of Li_2C_2.

To exclude that the formation of Li_2C_2 is induced by the Raman laser, i.e., an artifact of the measurement method, an alternative detection technique for Li_2C_2 has been applied. The SEI was hydrolyzed and the formed gases were investigated by mass spectrometry. The hydrolysis of Li_2C_2 leads to the formation of gaseous acetylene (H_2C_2) which gives an MS signal at 26 *m*/*z*. This signal was detected for the copper electrode after lithium plating as well for the copper electrode after lithium stripping. It can be concluded, that Li_2C_2 remains on the copper electrode after lithium is dissolved and that Li_2C_2 is formed independent of the use of a Raman laser.

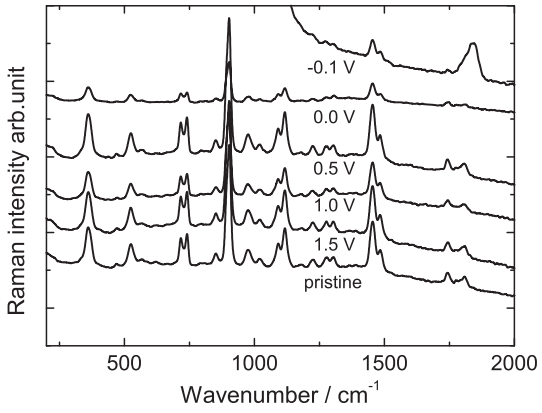

Fig. 7. Raman *in-situ* measurement of a copper electrode as working electrode with lithium as counter and reference electrode.

At contrast to the mapping for Li_2C_2 (shown in Fig. 5) the mapping for Li_2CO_3 (cf. Fig. 6) shows a more homogenous distribution.

To further investigate the process of SEI formation, an *in situ* Raman experiment was carried out (cf. Fig. 7). Up to a potential of 0.5 V vs. Li/Li^+ no changes in the Raman spectrum were observed. At 0 V vs. Li/Li^+ the intensities of signals representing the electrolyte decreased. However, no other signals were detected down to a potential of 0 V vs. Li/Li^+. By the use of *in situ* Raman spectroscopy we showed that Li_2C_2 forms at potentials below 0 V vs. Li/Li^+ and that this new method is suitable and helpful to investigate the SEI.

4. Conclusion

We showed that Li_2C_2 is a substantial part of the SEI which is formed on the surface of the lithium which is plated electrochemically on copper when 1 M $LiPF_6$ in EC:DEC (3:7, by wt.) is used as electrolyte. The existence of Li_2C_2 was further proven with a mass spectrometer. Acetylene gas was detected, when the copper foil with plated lithium was hydrolyzed. The distribution of Li_2C_2 and Li_2CO_3 was analyzed with Raman mapping. Li_2C_2 is primarily present on lithium deposits. The formation of Li_2C_2 starts below a potential of 0 V vs. Li/Li^+ which was proven via *in situ* Raman spectroscopy.

Acknowledgments

The authors gratefully acknowledge the financial support of this work by the DFG (German Research Foundation) as part of the research initiative PAK 177 “Funktionsmaterialien und Materialanalytik zu Lithium-Hochleistungsbatterien” (contract numbers

WI 2929/1-1 and WI 2929/5-1) on materials for lithium ion batteries.

References

[1] M. Winter, S. Passerini, in: Telecommunications Energy Conference (INTELEC), 2011 IEEE 33rd International, 2011.
[2] J.O. Besenhard, M. Winter, Pure and Applied Chemistry 70 (1998) 603–608.
[3] J.O. Besenhard, M. Winter, Chemphyschem 3 (2002) 155.
[4] J.O. Besenhard, M. Winter, Chemie in Unserer Zeit 33 (1999) 14.
[5] J.O. Besenhard, M.W. Wagner, M. Winter, A.D. Jannakoudakis, P.D. Jannakoudakis, E. Theodoridou, Journal of Power Sources 44 (1993) 413–420.
[6] R.D. Rauh, S.B. Brummer, Electrochimica Acta 22 (1977) 75–83.
[7] R. Selim, P. Bro, Journal of the Electrochemical Society 121 (1974) 1457–1459.
[8] A.J. Parker, P. Singh, E.J. Frazer, Journal of Power Sources 10 (1983) 1–11.
[9] Y. Sasaki, M. Hosoya, M. Handa, Journal of Power Sources 68 (1997) 492–496.
[10] D. Aurbach, Y. Gofer, M. Ben-Zion, P. Aped, Journal of Electroanalytical Chemistry 339 (1992) 451–471.
[11] M. Winter, J.O. Besenhard, M.E. Spahr, P. Novak, Advanced Materials 10 (1998) 725–763.
[12] M. Winter, W. Appel, B. Evers, T. Hodal, K. Moller, I. Schneider, M. Wachtler, M. Wagner, G. Wrodnigg, J. Besenhard, Monatshefte fuer Chemie 132 (2001) 473–486.
[13] M.R. Wagner, P.R. Raimann, A. Trifonova, K.C. Moeller, J.O. Besenhard, M. Winter, Electrochemical and Solid State Letters 7 (2004) A201–A205.
[14] K. Tasaki, A. Goldberg, M. Winter, Electrochimica Acta 56 (2011) 10424–10435.
[15] P. Verma, P. Maire, P. Novak, Electrochimica Acta 55 (2010) 6332–6341.
[16] M. Winter, K.-C. Möller, J.O. Besenhard, SEI Formation in Li Batteries – I. General Principles, in: Z. Stoynov, D. Vladikova (Eds.), Portable and Emergency Energy Sources, Prof. Marin Drinov Publishing House, Sofia, 2006, pp. 101–116.
[17] H.J. Santner, K.C. Moller, J. Ivanco, M.G. Ramsey, F.P. Netzer, S. Yamaguchi, J.O. Besenhard, M. Winter, Journal of Power Sources 119 (2003) 368–372.
[18] K.C. Moller, H.J. Santner, W. Kern, S. Yamaguchi, J.O. Besenhard, M. Winter, Journal of Power Sources 119 (2003) 561–566.
[19] E.C. Le Ru, P.G. Etchegoin, Principles of Surface-enhanced Raman Spectroscopy and Related Plasmonic Effects, Elsevier, Amsterdam, 2009.
[20] Handbook of Optical Constants of Solids III, Academic Press, New York, 1998.
[21] M.G. Albrecht, J.A. Creighton, Journal of the American Chemical Society 99 (1977) 5215–5217.
[22] R. Schmitz, R. Müller, S. Krüger, R.W. Schmitz, S. Nowak, S. Passerini, M. Winter, C. Schreiner, Journal of Power Sources 217 (2012) 98–101.
[23] U. Ruschewitz, R. Pottgen, Zeitschrift Fur Anorganische Und Allgemeine Chemie 625 (1999) 1599–1603.
[24] N. Koura, S. Kohara, K. Takeuchi, S. Takahashi, L.A. Curtiss, M. Grimsditch, M.L. Saboungi, Journal of Molecular Structure 382 (1996) 163–169.
[25] D. Ostrovskii, M. Edvardsson, P. Jacobsson, Journal of Raman Spectroscopy 34 (2003) 40–49.
[26] G. Socrates, Infrared and Raman Characteristic Group Frequencies, third ed., John Wiley & Sons Ltd., Chichester, 2001.